Journal of Applied Fluid Mechanics, Vol. 10, No. 3, pp. 785-799, 2017.
Available online at www.jafmonline.net, ISSN 1735-3572, EISSN 1735-3645.
DOI: 10.18869/acadpub.jafm.73.240.26563

Numerical Studies on the Effect of Diffuser Rotational Speeds on Low Pressure Ratio Centrifugal Compressor Performance

S. Seralathan† and D. G. Roychowdhury

Hindustan Institute of Technology and Science, Padur, Tamilnadu, 603 103, India

†*Corresponding Author Email: siva.seralathan@gmail.com*

(Received May 18, 2016; accepted January 14, 2017)

ABSTRACT

Numerical investigations are conducted to analyze the effect of rotational speeds of rotating vaneless diffuser on performance of a low-pressure ratio centrifugal compressor stage at off-design and design flow coefficients. Four different rotational speeds are selected for the rotating vaneless diffuser. Free type rotating vaneless diffusers are rotated at speed ratios SR0.25, SR0.50 and SR0.75. Total temperature of the fluid at stage exit increases with increase in rotational speeds of the free rotating vaneless diffuser. This affects the efficiency of free rotating vaneless diffusers. Its flow angles are smaller resulting in a shorter flow path length thereby reducing the frictional losses substantially. Gain in stagnation pressure is observed for all free rotating vaneless diffuser configurations. The rotational speeds determine the extent of net gain in energy level of the fluid and drop in total pressure losses. Based on static and stagnation pressure distributions at stage exit, the flow in FreeRVDSR0.75 undergoes a comparatively better diffusion process. In general, efficacy of diffusion process in a compressor stage with free rotating vaneless diffuser is better at speed ratio above 0.50. Subsequently, the speed ratio is increased to SR1.0 thereby the rotating vaneless diffuser behave like a forced type. Various free rotating vaneless diffuser configurations are compared with the forced type of rotating vaneless diffuser. Based on this study, it is understood that an optimum rotational speed of the rotating vaneless diffuser plays an important role in facilitating the effective diffusion process within the diffuser passage.

Keywords: Centrifugal compressor; Shrouded type impeller; Rotational speed; Vaneless diffuser; Rotating; Stationary.

NOMENCLATURE

b	blade width
C	absolute velocity
C_{po}	stagnation pressure coefficient
C_m	meridional velocity
C_p	static pressure coefficient
P_o	stagnation pressure
P	static pressure
R	radius ratio
r	radius
W	specific work
U	impeller tip speed
X	non-dimensionalised axial distance
x	axial distance
ψ_{loss}	stagnation pressure loss coefficient
ψ_p	static pressure recovery coefficient
Φ	flow coefficient
ψ	energy coefficient
ρ	air density
α	flow angle (in degrees)
η_{isen}	isentropic efficiency
1	inlet of the impeller
2	exit of the impeller
3	inlet of stationary vaneless diffuser
4	exit of stationary vaneless diffuser
3^*	free rotating vaneless diffuser inlet
4^*	free rotating vaneless diffuser exit
FreeRVD	shrouded impeller with free rotating vaneless diffuser of diffuser diameter ratio 1.40
SR	speed ratio
SR1.0	free rotating vaneless diffuser rotating at a speed equal to the impeller's rotational speed
SR0.75	free rotating vaneless diffuser rotating at ¾th speed of the impeller's rotational speed
SR0.50	free rotating vaneless diffuser rotating at ½ speed of the impeller's rotational speed

SR0.25 free rotating vaneless diffuser rotating at ¼th speed of the impeller's rotational speed

SVD shrouded impeller with stationary vaneless diffuser of diffuser diameter ratio 1.40

1. BACKGROUND AND OBJECTIVE

In the conventional stationary vaneless diffuser, walls of the diffuser are not rotating. As the diffusion process occur within the passage of diffuser, energy transformation happens in the form of rise in static pressure. However, within the diffuser passage, the flow undergoes losses due to friction occurring with the stationary walls of diffuser. Moreover, the flow leaving the centrifugal impeller is highly non-uniform in nature with presence of separated zones i.e., jets and wakes. These different energy level zones undergo mixing immediately after the entry into the vaneless diffuser and proceed in radial direction of the diffuser passage. Thus, mixing loss and frictional loss lead to a considerable loss of stagnation pressure that occurs between the diffuser inlet and exit. These losses form a major part of the stagnation pressure loss in conventional stationary vaneless diffuser. Hence, novel approach in design and development of diffusion systems are needed to overcome these losses. One such approach is to rotate the existing stationary vaneless diffuser at a speed which is fraction to impeller's rotational speed and this type is termed as free rotating vaneless diffuser.

In the early 1970's, Raymond Castaing (1972) suggested to rotate the vaneless diffuser used in the high-pressure ratio centrifugal compressors. The idea was to make the walls of the vaneless diffuser to rotate independently at an angular speed nearly half the impeller's rotational speed. Due this arrangement, the frictional losses were expected to be reduced substantially along with an increase in static pressure recovery, more uniform flow angle and velocity profile of the absolute flow at exit of the independently / free rotating vaneless diffuser. This arrangement retained the existing advantages of conventional vaneless diffuser. Based on this observation by Raymond Castaing, Fradin (1975) studied the effect of rotational speed of a vaneless diffuser on the performance of a centrifugal compressor. Losses due to fluid friction got reduced by making the walls of the diffuser to rotate at an angular velocity lesser than that of an impeller. Fradin concluded that the diffuser efficiency improved by 25% and overall efficiency of the compressor by 2% to 5%. Rodgers and Mnew (1970; 1974; 1975) as well as Rodgers (1972; 1974; 1976) carried out studies on using free rotating vaneless diffuser for the centrifugal compressor with active support from U.S. Army MERDC. Initial findings showed that free rotating vaneless diffuser was mechanically feasible and aerodynamically effective. Subsequently, Rodgers and Mnew (1975) as well as Rodgers and Blinman (1977) carried out experimental investigations on a model free rotating vaneless diffuser of a high pressure ratio single stage centrifugal compressor. The comparative studies were carried out under braked condition (i.e., as a stationary vaneless diffuser) and free rotating conditions as a free rotating vaneless diffuser. Under free rotating conditions, the diffuser performance improved a lot. The frictional losses reduced by almost 70% and overall static pressure recovery improved by 22% by rotating the free vaneless diffuser section at speed ratios above 0.40. The overall compressor efficiency also increased around four to five percent. The non-uniform entry flow profiles to the diffuser was smoothed out by the presence of free rotating vaneless diffuser, thereby enabling a wider flow range with better performance for the subsequent downstream diffusion systems.

This concept of rotating the walls of a vaneless diffuser was tried much earlier by the designers of pumps. Novak (1907) used this free rotating vaneless diffuser concept in a centrifugal pump operating at low-Reynolds numbers and reported a considerable improvement in the performance. Yves Ribaud and Christian Fradin (1989) took effort to revisit the researches on free rotating vaneless diffuser. They carried out reevaluation of the work done by Rodgers and Mnew (1970; 1974; 1975) and Fradin (1975) on free rotating vaneless diffusers. They emphasized again that the free rotating vaneless diffuser concept was mechanically feasible. Besides, there was a significant reduction in frictional loss along with an improved flow behavior. Yves Ribaud and Christian Fradin (1989) also suggested in experimenting newer types of rotating vaneless diffusers with respect to low specific speed centrifugal compressors. Recently, Seralathan and Roy Chowdhury (2014a; 2015) carried out preliminary numerical investigations on a compressor stage consisting free rotating vaneless diffuser. The comparative studies were carried out on a compressor stage of diffuser diameter ratio 1.40 in which, the diffuser diameter ratio of the free rotating vaneless diffuser section is 1.30. The remaining downstream diffuser diameter ratio was taken care by a stationary vaneless diffuser. The studies were conducted by rotating the free rotating vaneless diffuser at varied speed ratios. Free rotating vaneless diffuser configurations produced higher static pressure rise and reduced stagnation pressure losses. The static pressure recovery of various free rotating vaneless diffusers increased over the entire flow range. The efficiencies of various free rotating vaneless diffuser configurations were observed to be marginally lesser by 3.5 to 5.3%.

Most of the earlier researches on free rotating vaneless diffusers were focused along with high pressure ratio centrifugal compressors. Few literatures are available in open source focusing on low pressure ratio centrifugal compressor stage with free rotating vaneless diffuser. Based on the literature review, it is understood that there is no

Table 1 Specification details

Centrifugal impeller - Shrouded type (Govardhan *et al.* 1978)							
Diameter at exit of the impeller	D_2	570 mm		Width of the blade at exit	b_2	27.6 mm	
Diameter at inlet of the impeller	D_1	215.2 mm		Width of the blade at inlet	b_1	58.5 mm	
Outer diameter to inner diameter ratio	D_2/D_1	2.649		Thickness of the blade	T	6 mm	
Diameter at exit of the impeller disks	D_2''	570 mm		Blade angle at the exit	β_2	90°	
Diameter at exit of the impeller blade	D_2'	570 mm		Blade angle at the inlet	β_1	44.6°	
Rotational speed of the impeller	N	1500 rpm		Number of blades	Z	18	
Free rotating vaneless diffuser (FreeRVD)				Stationary vaneless diffuser (SVD)			
Diffuser diameter ratio	D_4^*/D_3^*	1.40		Diffuser diameter ratio	D_4/D_3	1.40	
Inlet diameter of diffuser	D_3^*	570 mm		Inlet diameter of diffuser	D_3	570 mm	
Outlet diameter of diffuser	D_4^*	798 mm		Outlet diameter of diffuser	D_4	798 mm	
Rotational speed of FreeRVD							
SR0.25 = 375 rpm	SR0.50 = 750 rpm		SR0.75 = 1125 rpm		SR1.0 = 1500 rpm		

published literature on replacing fully the existing conventional stationary vaneless diffuser with a free rotating vaneless diffuser of equivalent diffuser diameter ratio in a low-pressure ratio centrifugal compressors stage.

A low-pressure ratio single stage centrifugal compressor having a shrouded type centrifugal impeller with diffuser of diffuser diameter ratio 1.40 is chosen for the present numerical investigations. Three different rotational speeds are selected for the free rotating vaneless diffuser. The rotational speeds of free rotating vaneless diffuser are maintained at 0.25 times (FreeRVDSR0.25), 0.50 times (FreeRVDSR0.50) and 0.75 times (FreeRVDSR0.75) the rotational speed of the shrouded impeller. Later, the rotational speed of this rotating vaneless diffuser is enhanced and it is kept equal to that of impeller's rotational speed (FreeRVDSR1.0). The objectives of the present study are:

- To analyze the effect of rotational speeds of a rotating vaneless diffuser on flow diffusion using various flow parameters and performance characteristics parameters.
- Comparing the performance of the compressor stage having different free rotating vaneless diffusers (FreeRVDSR0.25, FreeRVDSR0.50 and FreeRVDSR0.75) with a compressor stage having a forced type of rotating vaneless diffuser (FreeRVDSR1.0).

Moreover, all the results are compared with the conventional stationary vaneless diffuser (SVD).

2. NUMERICAL METHODOLOGY

The specification details of radial tipped shrouded type centrifugal impeller (Govardhan et *al.* 1978) are given in Table 1. The geometric model of impeller with stationary vaneless diffuser in the downstream of diffuser diameter ratio (D_4/D_3) 1.40 (SVD) is created. This is used as the base reference for evaluating the various rotating vaneless diffuser configurations considered for the present studies.

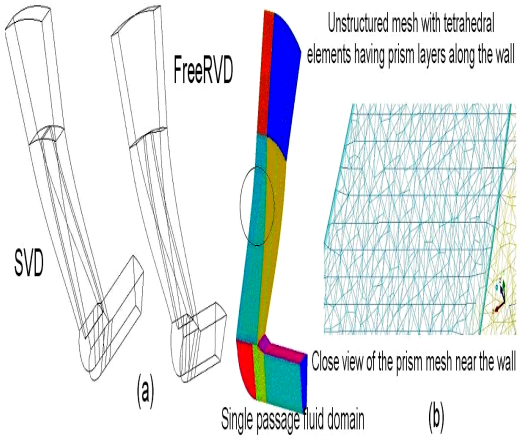

Fig. 1. (a) Computational geometry (b) Unstructured grid generation.

This same impeller is again modeled with a rotating vaneless diffuser in the downstream of diffuser diameter ratio 1.40 (FreeRVD). The specification details of the centrifugal compressor stage are given in Table 1. The numerical investigations on various configurations modeled above are carried out for a flow range ranging from design flow coefficient, $\Phi = 0.275$ to above off-design flow coefficients at $\Phi = 0.309$, 0.343 and 0.371. Fig. 1(a) shows the computational domains of FreeRVD and SVD configuration. The computational domain for the present studies consist a shrouded type impeller with blade and diffuser (rotating vaneless diffuser or stationary vaneless diffuser). The simulation of full impeller with blades along with diffuser involves huge computational resources as well as time. To avoid this, single passage approach is used as seen in Fig. 1(a) in modeling the computational

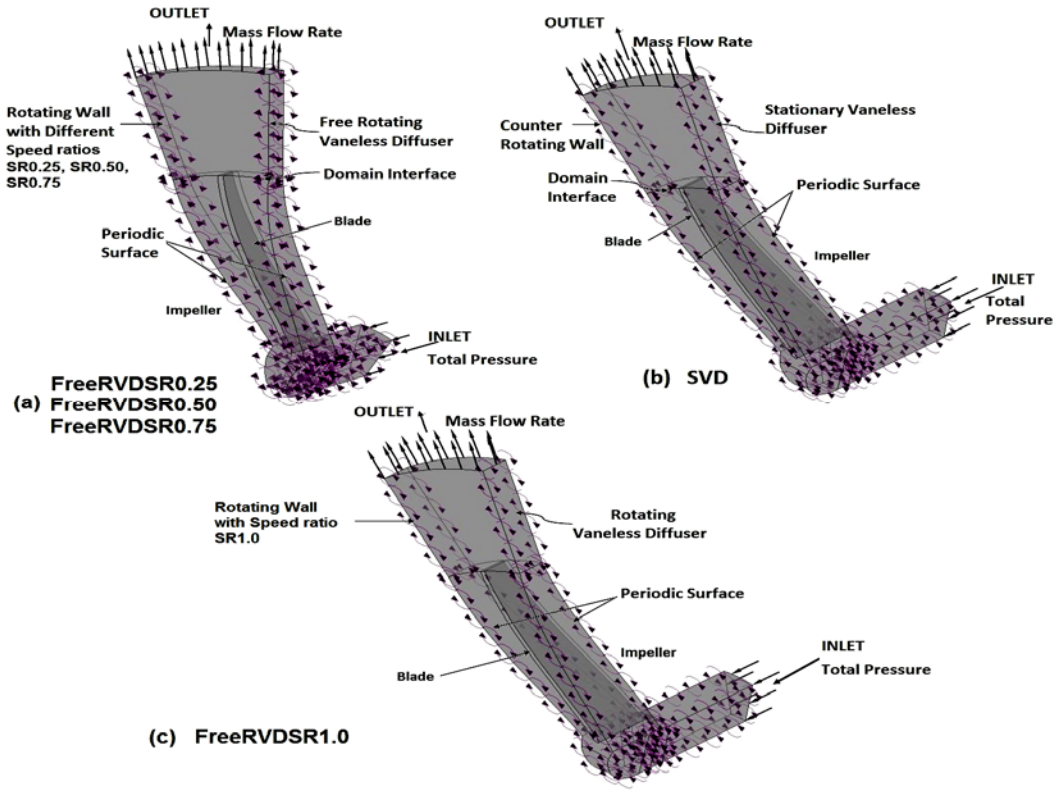

Fig. 2. Boundary conditions for the computational domain of FreeRVD and SVD configurations.

domain by treating the flow to be periodic in each impeller's blade passage. The geometric modeling and grid generation of the computational domain is carried out by using ANSYS ICEM CFD 13.0. Fig. 1(b) shows the generated mesh in the computational domain. Unstructured grid based on tetrahedral elements are generated along with fine elements i.e., prism shaped cells in the near-wall zones. This is done in order to achieve finer resolution in the boundary layer regions. The prism layered cells are introduced nearer to the hub wall as well as nearer to the shroud wall of shrouded type impeller, around the impeller's blade and nearer to the walls of diffuser (rotating vaneless diffuser / stationary vaneless diffuser). Based on the turbulence model requirements, the mesh is generated in the near wall zones and accordingly, a minimum y^+ value of 0.10 and maximum y^+ value of 1.0 are maintained at all the wall regions. In this present studies, as seen in Fig. 1(b), a minimum of seven to eight prism layered cells are kept in the near wall regions. To ensure that the numerical results are not dependent of generated mesh, grid independency study is performed. Table 2 and 3 shows the grid independency studies for SVD and FreeRVD configuration. With reference to grid G1, the percentage difference for grid G2 is less and grid G2 is taken up for the present studies. Based on this study, the total count of elements are 899833 including tetrahedral and prism for both FreeRVD and SVD configurations.

Table 2 Grid independency study for SVD

Grid (G)	Nodes	Elements	C_p	Difference in %
G1	335304	1042798	0.849	---
G2	240444	899833	0.843	0.706%
G3	173866	572403	0.831	2.120%

Table 3 Grid independency study for FreeRVD

Grid (G)	Nodes	Elements	C_p	Difference in %
G1	335304	1042798	0.982	---
G2	240444	899833	0.975	0.712%
G3	173866	572403	0.962	2.036%

As standard k-ε model lacks accuracy in prediction of separation and missing of transport effects, standard k-ω (Wilcox) as well as k-ω based Shear Stress Transport (SST Mentor) turbulence models are the most well known models used in turbomachinery depending upon the underlying flow regimes and levels of accuracy required. The numerical results obtained under steady-state conditions based on these turbulence models are compared with the available experimental results done by Govardhan *et al.* (1978). Values obtained with standard k-ω turbulence model are nearer to the values measured under experimental conditions and it is not shown here for the sake of brevity

(Seralathan Sivamani and Roy Chowdhury 2014b; Seralathan Sivamani and Roy Chowdhury 2016). Therefore, subsequent numerical studies are carried out by using this turbulence model. The numerical investigations are performed using commercial CFD code, ANSYS CFX 13.0, which solves the full three dimensional Reynolds Averaged Navier Stokes Equations based on finite volume method. The details of the boundary conditions imposed in the present studies are shown in Fig. 2. The boundary at inlet of the computational domain is shifted to the front by half the impeller's chord length from eye of the impeller. This is done to make certain that the effects of back pressure of impeller blade are not affecting the boundary condition at inlet. As the centrifugal compressor is a domain of rotating type, rotating frame of reference is imposed on the entire computational domain. At inlet, the total pressure is specified along with uniform inflow direction normal to its inlet plane as the boundary condition. The reference pressure mentioned is 1.01325 x 10^5 kPa. Hence, at inlet, the relative total pressure is zero Pascal. Air at 25^0C is specified as the fluid for the present studies. Standard k-ω (Wilcox) is used as the turbulence model and turbulence intensity of 5% is specified at the inlet. Rotational periodic boundary conditions are imposed at either side walls of the computational domain. Mass flow rate is specified as the boundary condition at the outlet based on the number of impeller blade passages present within the computational domain. In this study, the SVD computational domain consists of a stationary domain (i.e., stationary vaneless diffuser) and a rotating domain (i.e., impeller). In the stationary frame of reference, the walls of the vaneless diffuser do not rotate. Therefore, the stationary domain is imposed with a counter-rotating type boundary condition. Appropriate interface is kept in between the impeller and stationary vaneless diffuser to connect the meshes of these domains together across the frame change. For the present steady state simulation studies, frozen rotor interface is chosen for the rotor-stator frame change interface. This interface is robust and utilizes minimum computer resources. Similarly, for free rotating vaneless diffuser configurations namely, FreeRVDSR0.25, FreeRVDSR0.50 as well as FreeRVDSR0.75 configurations, the frozen rotor interface is introduced in between the rotating domain (i.e., impeller) and another rotating domain rotating with a different rotational speed (i.e., free rotating vaneless diffuser). The rotational speed of free rotating vaneless diffuser specified is a fraction with respect to impeller's rotational speed. FreeRVDSR1.0 configuration is rotating at the same rotational speed equivalent to that of the computational domain.

The shroud and hub of the impeller, blade as well as the stationary vaneless diffuser and rotating vaneless diffuser are imposed with wall boundary condition along with no slip condition. The wall roughnesses are ignored by considering it as a smooth wall. Automatic time steps are imposed for all the governing equation with a time step value equal to 0.2/ω, where 'ω' is defined as the angular velocity in rad/sec. Coupled solver is used and the computations of the steady state solutions are carried out till the residual values are converged. The normalized residuals in general are given by $\left[\tilde{r}_{\varphi}\right]=\frac{\left[r_{\varphi}\right]}{a_p \Delta\varphi}$, where r_φ is the raw residual control volume imbalance, a_p is the representative of control volume coefficient and $\Delta\varphi$ is the representative range of the variable in domain. The convergence criteria of RMS (root mean square) normalized values of all the governing equation residuals are set to 1 x 10^{-4}.

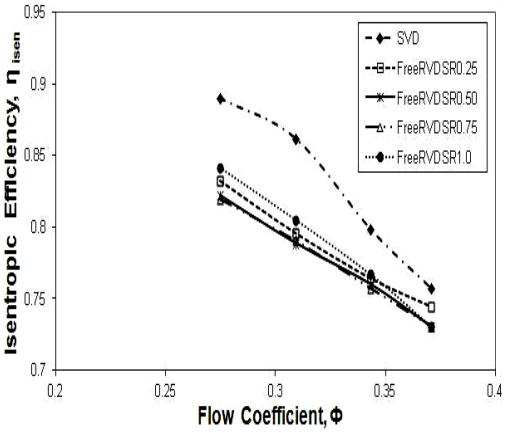

Fig. 3. Variations of isentropic efficiency with flow coefficients.

3. RESULTS AND DISCUSSION

3.1 Comparison of Various Free Rotating Vaneless Diffusers with Conventional Stationary Vaneless Diffuser

3.1.1 Effect on Compressor Stage Performance

Figure 3 shows the variations of efficiency against flow coefficient for various diffuser configurations. It is found that the efficiency of SVD is highest for the entire flow range. Efficiencies of free rotating vaneless diffuser (FRVD) configurations at different speed ratios are lesser compared to SVD. In general, it is observed that efficiencies of all the diffuser configurations decrease with increase in mass flow rate. Also, the decrease in efficiency for the entire flow range is maximum for SVD configuration. The efficiency of FreeRVDSR0.25 is slightly higher by 0.90% to 1.98% for the entire flow range compared to FreeRVDSR0.50 as well as FreeRVDSR0.75 and the efficiencies of the latter are nearly identical. The basis for various FRVD configurations realizing a lesser efficiencies is due to disk friction losses. Rotating the vaneless diffusers independently at different speed ratios result in increased disk friction losses. It is known that disk friction loss is a parasitic loss which results in raising the total temperature of fluid at stage exit. On close observation of various FRVD

configurations, it is found that the total temperature of fluid at stage exit increases with increase in speed ratio of free rotating vaneless diffuser from 0.25 to 0.75. This results with FreeRVDSR0.75 recording the least efficiency. Even though increased stagnation pressure distribution (as seen in Fig. 12 which is discussed later) is obtained with the compressor stage having free rotating vaneless diffusers, the fall in efficiency levels is the effect of it.

Energy coefficient values point out the energy obtained by the fluid as it flows through the centrifugal compressor stage. It is also a pointer for static pressure rise within the compressor stage. Fig. 4 shows the variations of stage energy coefficient against flow coefficients for various diffuser configurations. The energy coefficient values for SVD is the least. The energy coefficient of FreeRVDSR0.75 is highest by 38.10% to 46.04% compared to SVD and followed by FRVD configuration, FreeRVDSR0.50, which is higher by 28.91% to 35.53% and FreeRVDSR0.25 respectively.

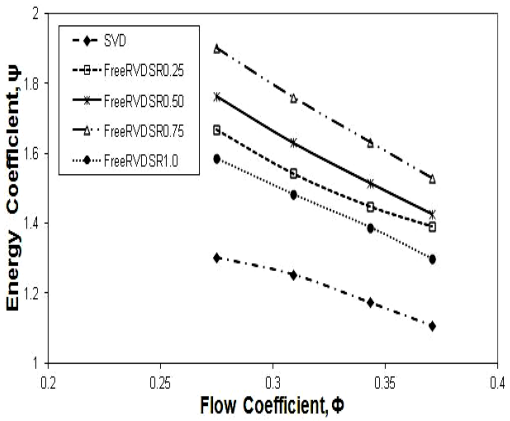

Fig. 4. Variations of energy coefficient with flow coefficients.

3.1.2 Effect on Diffuser Performance

Figure 5 shows the variation of static pressure recovery coefficients against flow coefficients. In general, the static pressure recovery coefficient values of various free rotating vaneless diffusers are higher compared to SVD by 25.37% to 51.58%. At design flow condition, the recovery of static pressure for FreeRVDSR0.25 improved by 51.58% compared to SVD. It is also improved for FreeRVDSR0.50 by 43.34% and 42.10% for FreeRVDSR0.75 respectively. The static pressure recovery coefficient of SVD increases gradually as the mass flow rate is increased, whereas for all FRVD configurations, recovery of static pressure is highest at design flow coefficient. It decreases gradually up to off-design flow coefficient, Φ = 0.309 and then it rises slightly and falls at other off-design flow coefficients. This may be due to minor variations in the realized stagnation pressure at diffuser entry region. Also, the maximum recovery of static pressure realized at design flow condition is due to comparatively higher additional energy added to the fluid (as seen in Fig. 7 at location R = 1.577) along with effective diffusion process within the diffuser passage (as seen in Fig. 14 at R = 1.577) which is discussed later. Moreover, the pattern of variation between SVD and various FRVD configurations, as seen in Fig. 5, for various flow coefficients correlates well with the static pressure distribution as shown in Fig. 14 at location R = 1.577. A superior recovery of static pressure by free rotating vaneless diffuser leads to an improved rise in static pressure (as observed in Fig. 14 and discussed later). This is a pointer towards the efficacy of diffusion process which is observed to be better in FRVD configurations compared to SVD.

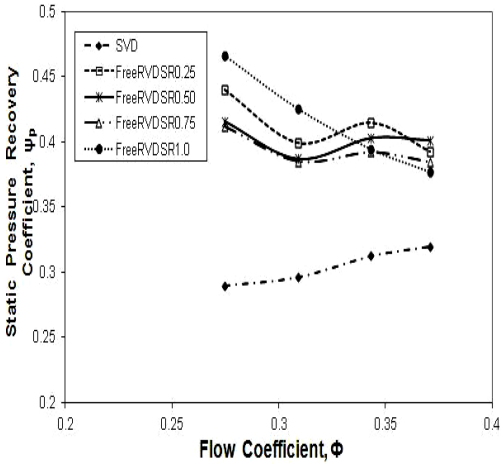

Fig. 5. Variations of static pressure recovery coefficient with flow coefficients.

Stagnation pressure loss coefficient is a pointer about the losses occurring within flow passage between the diffuser inlet and exit. Mixing of fluid with different energy levels and losses due to friction between the walls and flow are the major contributor for stagnation pressure losses. Fig. 6 shows the variations of stagnation pressure loss coefficients against flow coefficients. In the SVD, the loss of stagnation pressure is observed and this loss reduces gradually as the flow rate is increased under off-design flow conditions. A closer look into Fig. 6 reveals that there is no loss of stagnation pressure for various FRVD configurations at design as well as at off-design flow conditions. Rather, there is only gain in energy. The gain in total pressure is maximum at design flow condition, Φ = 0.275 for various FRVD configurations and this gain reduces with increase in mass flow rates. In the conventional vaneless diffuser (SVD), the diffuser walls are fixed and not rotating. The major contributor of total pressure losses of the flow is the fluid friction occurring with the stationary vaneless diffuser walls having a significant boundary layer growth. In a FRVD, as highlighted by Rodgers and Mnew (1975), the shear forces between the rotating vaneless diffuser walls and flow is significantly reduced. Also, the growth of boundary layer formation within this FRVD is much smaller

compared to stationary vaneless diffuser. This leads to a drastic reduction in losses. So, the presence of FRVD in the compressor stage, as in the present studies, helps in reducing substantially the frictional losses associated due to diffusion and this correlated well with the findings of Fradin (1975) and Rodgers and Mnew (1975). Also, the rotational speed at which the FRVD is rotated determines the extent of total pressure losses. As seen in Fig. 6, a gain in total pressure by 74.14% to 305.64% is observed for the entire flow range by increasing the speed ratio of free rotating vaneless diffuser from SR0.25 to SR0.50. Similarly, a gain of around 61.04% to 110.74% is also observed by increasing the speed ratio from SR0.50 to SR0.75. This is due to effective diffusion process occurring within the diffuser passages which could be correlated with the stagnation pressure distribution as shown in Fig. 12 which is discussed later. Also, the values of stagnation pressure loss coefficients (ψ_{loss}) are negative for all the flow coefficients. As it is known that a positive increase in ψ_{loss} values is a pointer towards increase in stagnation pressure loss, but these negative values of ψ_{loss} is an indication of gain in stagnation pressure. This gain in stagnation pressure achieved by effective diffusion is due to the energy added to the fluid which causes its kinetic energy level to rise. Also, this net gain in energy is achieved after overcoming the frictional losses due to walls. This net gain in energy levels reduces gradually due to increase in frictional losses within the diffuser passages with increase in mass flow rates. This investigation indicates that presence of FRVD reduces the stagnation pressure losses substantially resulting in net gain in kinetic energy level of the fluid in a compressor stage. Also, the speed ratios at which the FRVD is rotated determine the extent of net gain in energy level of the fluid.

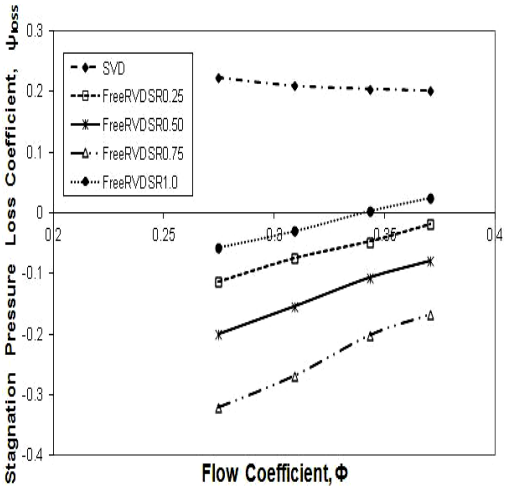

Fig. 6. Variations of stagnation pressure loss coefficient for different diffuser configurations.

3.1.3 Effect on Flow Parameters

The mass averaged absolute velocity distribution between hub and shroud walls of the diffuser with flow coefficients from diffuser inlet to exit measured at different radius ratio levels are shown in Fig. 7. As the radius ratios increases with radial locations, due to diffusion process, the absolute velocity reduces for SVD configuration. In a typical stationary vaneless diffuser, the difference in absolute velocities between inlet and exit of the diffuser gives an idea about the energy transformation occurring within the diffuser passage which results in as rise in static pressure. In case of FRVD, this may not be true as work input is added by the rotating walls of the diffuser. This can be visualized by comparing the contours of absolute velocities close to the wall locations (x/b = 0.10 and 0.90) as shown in Fig. 8. As the walls of the vaneless diffuser rotate, the fluid nearer to the walls also rotates with equivalent angular velocities. Also, the extent of fluid getting energized depends upon the rotational speed of FRVDs. It is observed that the rise in kinetic energy level of FreeRVDSR0.75 is maximum, which transforms itself into improved dynamic head by diffusion process. This is well observed in the form of increased stagnation pressure distribution for FreeRVDSR0.75 as seen in Fig. 12, which is discussed later.

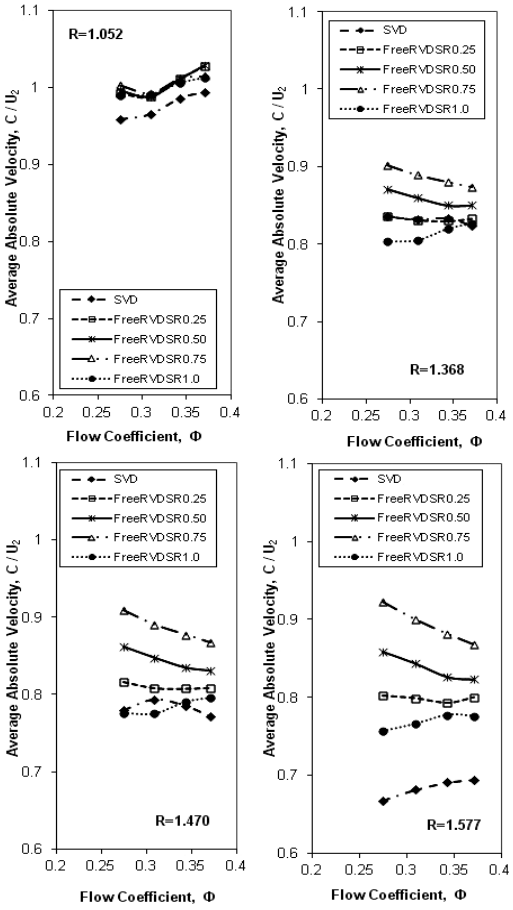

Fig. 7. Variation of non dimensional mass averaged absolute velocity with flow coefficient.

Also, a closer look into the absolute velocity contours at mid plane location, x/b = 0.50, 0.40 and 0.60 in Fig. 8 reveals the extent of fluid getting energized in various FRVD configurations. The

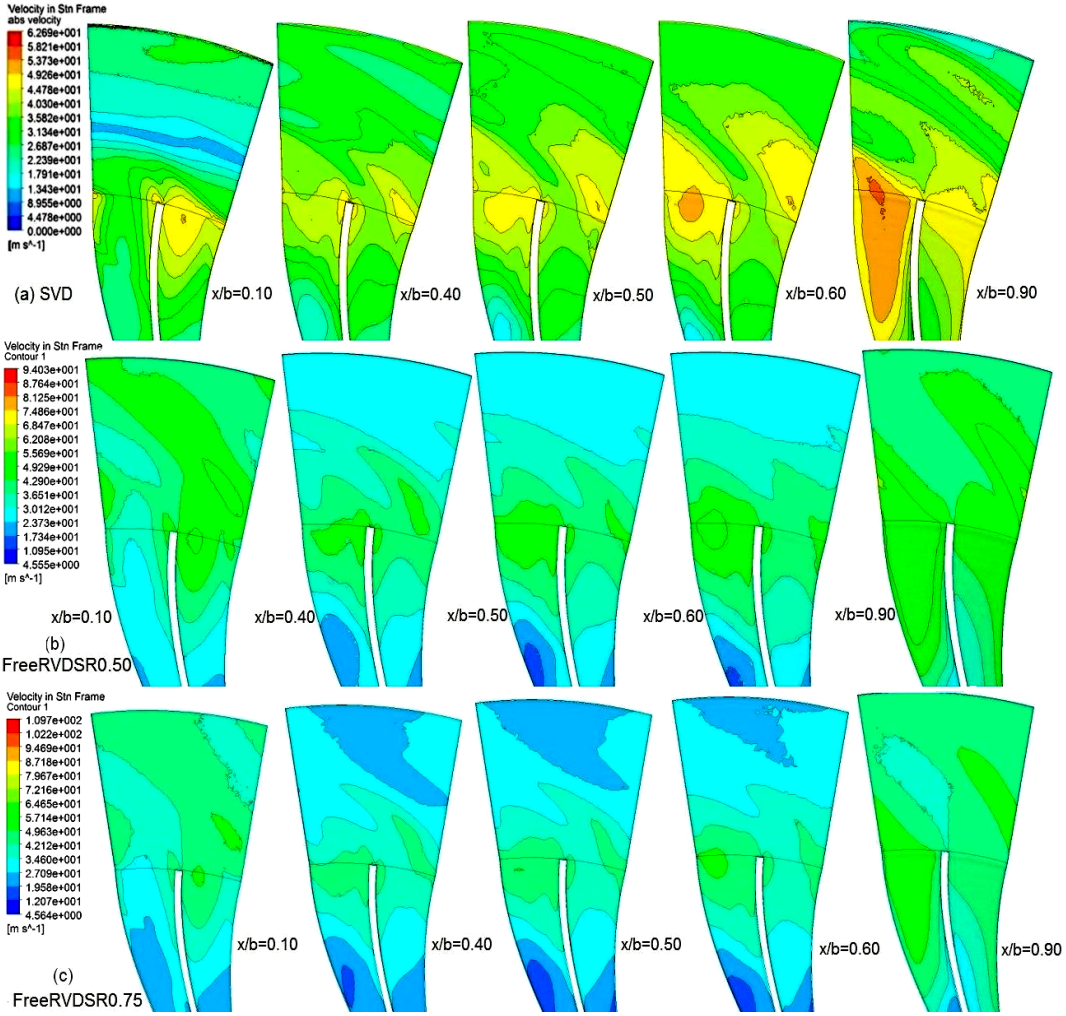

Fig. 8. Distribution of absolute velocity axially from hub to shroud at Φ = 0.275 for FreeRVD and SVD configurations.

absolute velocity gradually reduces towards the mid stream location from walls of the diffuser. This is due to gradual variations in angular velocities of the fluid away from the free rotating diffuser walls. These are again exemplified with the meridional view plots as seen in Fig. 9. It can be noted that at entry region of the diffuser (R = 1.052), as seen in Fig. 7, the absolute velocities of all FRVD configurations are higher than SVD. The absolute velocities of all configurations increase with increase in mass flow rates. Subsequently, as observed at radius ratios R = 1.368 and above, the absolute velocities of free rotating diffuser configurations namely, FreeRVDSR0.50 and FreeRVDSR0.75 decreases gradually with increase in mass flow rate. On the other hand, for FreeRVDSR0.25, the absolute velocity distributions remain nearly constant at all flow rates. As pointed out by Yves Ribuad and Christian Fradin (1989), the basic concept behind the FRVD is to balance the friction torque due to main flow within the diffuser passage with the resisting torque of fluid confined adjacent to rear part of the rotating diffuser. In this present study, the diffuser diameter ratio of free rotating vaneless diffuser is fixed. In general, as the rotational speeds of rotating vaneless diffuser are increased, the losses due to disk friction increases and with the increase in mass flow rate, the contribution by disk friction loss decreases. As disk friction loss is a parasitic loss, only actual work input is added to the FRVD section in causing energy transfer and raising the energy level of the fluid. This clearly depends upon the speed ratio of free rotating vaneless diffuser section. The mass flow rates also determine this energy transfer and rise in energy level. This is evident from the increase of absolute velocity with increase in speed ratio at R = 1.577. By comparing Fig. 7 and Fig. 12 at radius ratio R = 1.577 for design flow coefficient, it is observed that the efficacy of diffusion process is better in FRVD and it improves with increase in rotational speed ratio from SR0.25 to SR0.75. The mass flow rate determines the energy transfer and rise in energy level of fluid within the free rotating vaneless diffuser section. Therefore, at above off-design flow conditions, the realized absolute velocity after diffusion process at R = 1.577 decreases with increase in mass flow rate. As the increase in energy level of the fluid along with process of diffusion in FreeRVDSR0.25 is inferior

compared to SR0.50 and SR0.75, the absolute velocity distributions remain nearly constant at all flow rates. Fig. 9 shows the meridional view plots of absolute velocity distribution at design flow condition, Φ = 0.275 for various configurations. In SVD, a recirculation region is observed immediately after the diffuser entry region along the hub side wall of stationary vaneless diffuser. This causes the distinct core flow to shift towards the shroud side and it diffuses as radius ratio increases. The diffusion process efficacy is determined by the reduction in values of absolute velocities. By comparing all the configurations as seen in Fig. 9 at diffuser exit, it is observed that the flow is not fully diffused in SVD. In FRVD configurations, the process of diffusion is better, but the effectiveness of diffusion process depends upon diffuser's rotational speed. Among all the FRVD configurations, FreeRVDSR0.75 reports better diffusion. These correlate well with the stagnation pressure and static pressure distribution as seen in Figs. 12 and 14 which are discussed later.

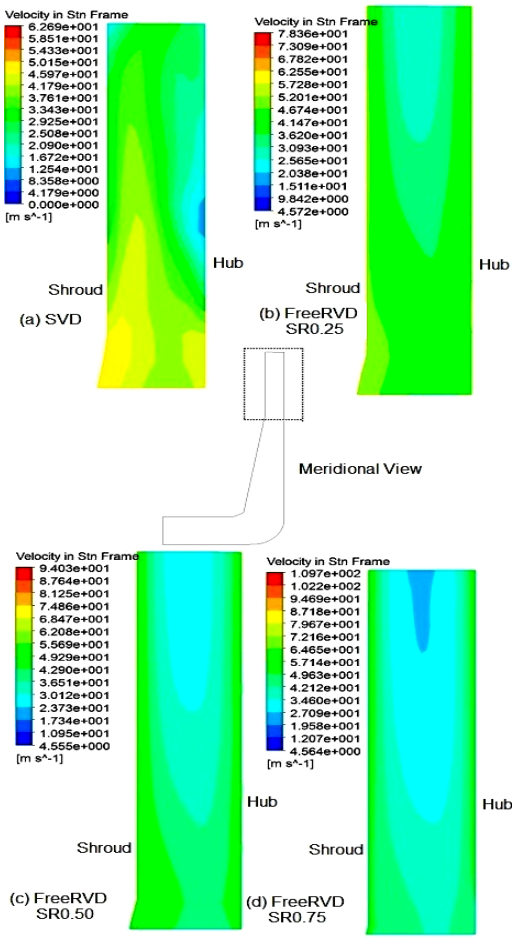

Fig. 9. Meridional view plots of absolute velocity distribution for various configurations.

Figure 10 shows the velocity vector plots on axial plane at mid axial position x/b = 0.50 for all configurations at design flow coefficient. The high-kinetic energy region (jet) and low-kinetic energy region (wake) are visible in all the configurations. A closer look of the flow reveals non-uniformity of the flow at impeller exit. In SVD, fluid with different energy level mixes inside the diffuser region and it continues further in the downstream. But, in free rotating vaneless diffusers, as seen in Fig. 10(b), 10(c) and 10(d), the mixing of fluid with different energy levels do not occur immediately inside the diffuser and occurs only later on in the downstream near exit. Furthermore, the rotational speed of diffuser impacts the rate of mixing process within the diffuser passage as seen in Fig. 10(b), 10(c) and 10(d). On comparing all the FRVD configurations, it can be seen that the mixing process is rapid, effective in FreeRVDSR0.75 and flow is observed to be uniform at diffuser exit. Mixing of fluid with different energy levels occurs within the diffuser passage during the progress of diffusion process. This causes a rise in static pressure but lead to a substantial loss of dynamic component of stagnation pressure. This inhibits further conversion of energy into static pressure by a suitable downstream diffusing component. Also, mixing losses is one of the sources for poor efficiency as it hampers effective diffusion. Based on the vectors plots as seen in Fig. 10, it is found that the presence of free rotating vaneless diffuser reduces the mixing losses considerably as the mixing takes place near the exit of diffuser and also, its rotational speed influences the mixing process. This can be correlated with the values of stagnation pressure loss coefficient as shown in Fig. 6 where the total pressure loss of FreeRVDSR0.75 is the least.

The mass averaged flow angle between hub and shroud walls of the diffuser with flow coefficients from diffuser inlet to exit are shown in Fig. 11. In general, the flow angle increases with increase in mass flow rates for all the diffuser configurations. As seen in Fig. 11, the flow angle for SVD increases along the radial direction and its flow angle is the highest in entire flow range. This causes the SVD to have a larger absolute flow path. So, the logarithmic path length of the flow traced by SVD configuration is more which directly results in higher frictional losses. This results in as higher stagnation pressure loss coefficient values as can be seen in Fig. 6. With the presence of FRVDs, the flow angle gradually decreases along the radial direction. Also, the rate of decrease varies slightly depending upon the rotational speed of FRVDs. FreeRVDSR0.75 has the lowest flow angles and FreeRVDSR0.25 has the highest. This is visualized in the velocity vector plots by comparing various FRVD configurations with SVD at mid axial position (x/b = 0.50). In a rotating vaneless diffuser, the logarithmic path length and dynamic head depends upon relative velocity i.e., its direction and magnitude of the flow within the diffuser. With a higher relative flow angle and smaller flow path length, the frictional losses are substantially reduced in free rotating vaneless diffusers. This is observed in Fig. 6. From this figure, it can be seen that the stagnation pressure loss coefficient is least for FreeRVDSR0.75 in comparison with SVD. It is then followed by FreeRVDSR0.50 and FreeRVDSR0.25 configurations.

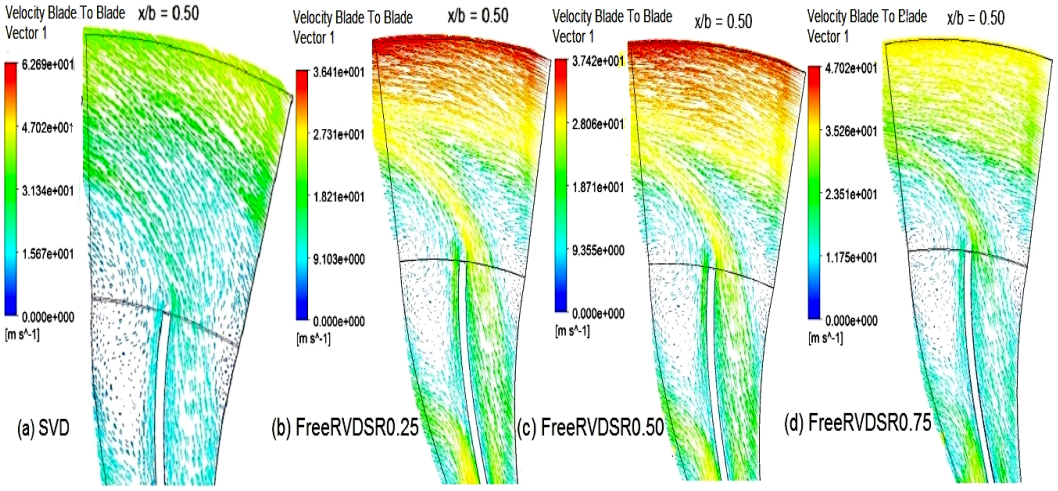

Fig. 10. Velocity vector plot at mid axial position for design flow coefficient.

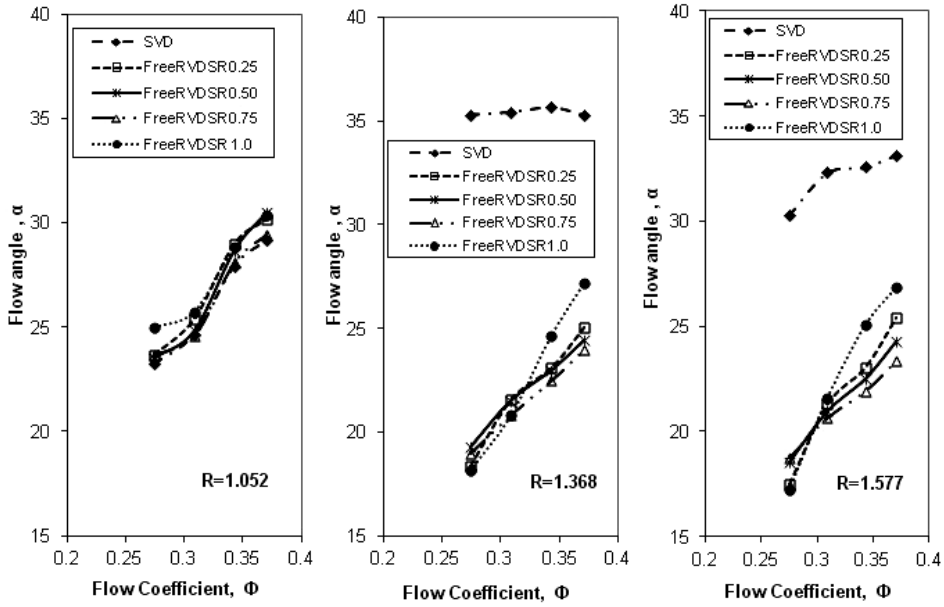

Fig. 11. Variations of flow angle with flow coefficients for various configurations.

The stagnation pressure reduces as the radius ratios increases with radial locations at various flow coefficients. Also, as the mass flow rate increases, the stagnation pressure decreases at all radial locations. The stagnation pressure drop is a pointer towards the quantity of losses occurring within the diffuser passage during diffusion process. The mass averaged stagnation pressure distribution between hub and shroud walls of the diffuser with flow coefficients from diffuser inlet to exit measured at different radius ratio levels are shown in Fig. 12 as dimensionless parameter $C_{po.}$ As observed at radius ratio R = 1.052 in Fig. 12, the stagnation pressure distribution of all free rotating vaneless diffusers are higher compared to SVD. Comparatively larger drop in stagnation pressure is occurring only for SVD configuration and this is mainly due to fluid friction with the walls. This trend is not observed in any of the FRVD configurations. In the conventional stationary vaneless diffuser (SVD), the diffuser walls are stationary. The boundary layer thickness is larger compared to free rotating vaneless diffuser section. This results into higher frictional losses between the diffuser walls and flow thereby leading to a significant drop in stagnation pressure. As the vaneless diffusers are rotated independently at different speed ratios, the frictional losses within the diffuser passage are reduced. This reduction in losses is also dependent upon the speed ratios of free rotating vaneless diffuser to which the formation of boundary layer thickness is also related. As seen in Fig. 12, among all the FRVD configurations, the stagnation pressure distribution for FreeRVDSR0.25 is the least. As observed in Fig. 12, the extent of dynamic head realized by diffusion depends upon the rotational speeds of FRVD, as the latter determines the extent of additional kinetic energy added to the fluid. The contours of stagnation pressure distribution at

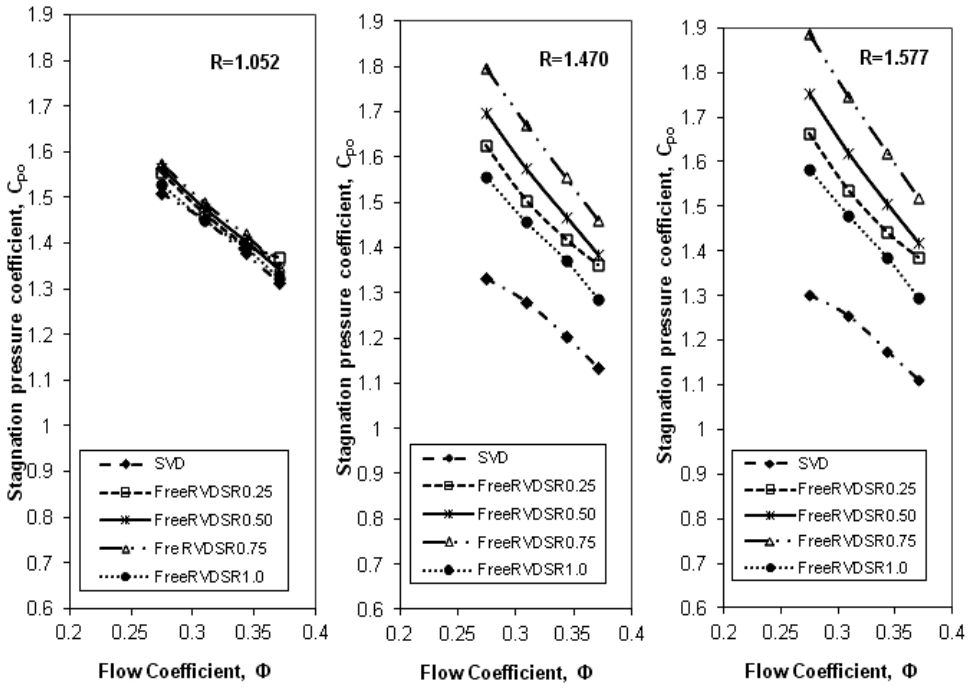

Fig. 12. Variations of stagnation pressure coefficient for different diffuser configurations.

Φ = 0.275 as shown in Fig. 13 reveals the same. The extent of kinetic energy added to the fluid gradually reduces towards the mid stream location away from the walls of rotating diffuser. This can be visualized in Fig. 13(b) and 13(c), where the stagnation pressure distribution at mid axial position (x/b = 0.50) is lower than the near wall locations (x/b = 0.10 and 0.90). By comparing the contours of stagnation pressure distributions of free rotating vaneless diffusers, it is clear that the magnitude of stagnation pressure distribution at exit of the compressor stage improves as the speed ratios of free rotating diffuser section is increased from speed ratio SR0.25 (which is presently not shown here) to SR0.75. As can be seen from Fig. 13, the stagnation pressure distribution at axial locations at x/b = 0.40, 0.50 and 0.60 is observed to be highly non-uniform for SVD configuration. Also, the flow is not fully diffused as observed at diffuser exit. By rotating the vaneless diffuser section at speed ratio SR0.25 (which is not shown here), the distribution pattern of stagnation pressure within the diffuser improves. However, the distribution pattern becomes more uniform with further increase in speed ratios. Based on these observations, it can be concluded that distorted flow profiles from the exit of impeller are smoothed out by the presence of free rotating vaneless diffuser thereby enhancing the overall compressor performance.

Figure 14 shows the mass averaged static pressure distribution between hub and shroud walls of the diffuser as dimensionless parameter C_p with flow coefficients from diffuser inlet to exit measured at different radius ratio levels. With increase in mass flow rates, the values of static pressure at any radial locations decreases. At the diffuser entry region (R = 1.052), the static pressure distribution of various free rotating vaneless diffusers are marginally lesser than SVD. The static pressure rise for all free rotating vaneless diffusers at location immediately to exit of diffuser (i.e., R = 1.470) are in close range with each other and varying in magnitude by around 1.97% at design flow condition and 1.22% to 5.49% at off design flow conditions. Nevertheless, the static pressure rise realized at R = 1.577 is higher compared to SVD by 17.12% at design mass flow rate and by around 11.05% to 14.46% at off design flow conditions. The contours of static pressure distribution taken from shroud to hub at axial direction for design flow coefficient are shown in Fig. 15. As the walls of free rotating vaneless diffusers are rotated at certain angular velocities based on speed ratios, the fluid with increased kinetic energy level transform itself into an increased static pressure rise by diffusion process as flow goes to next level of radius ratios. As observed in Fig. 15(a), the flow is not fully diffused in SVD at stage exit. Among all the free rotating vaneless diffusers, FreeRVDSR0.75 offers a better static pressure rise and closely followed by FreeRVDSR0.50. On comparing the static pressure distribution along with distribution of stagnation pressure at stage exit, it is found that FreeRVDSR0.75 undergoes a better diffusion process. This establishes the efficacy of diffusion process by the presence of FRVD in a compressor stage. The rate of diffusion improved in the compressor stage by rotating the free rotating vaneless diffuser section at speed ratios above SR0.50.

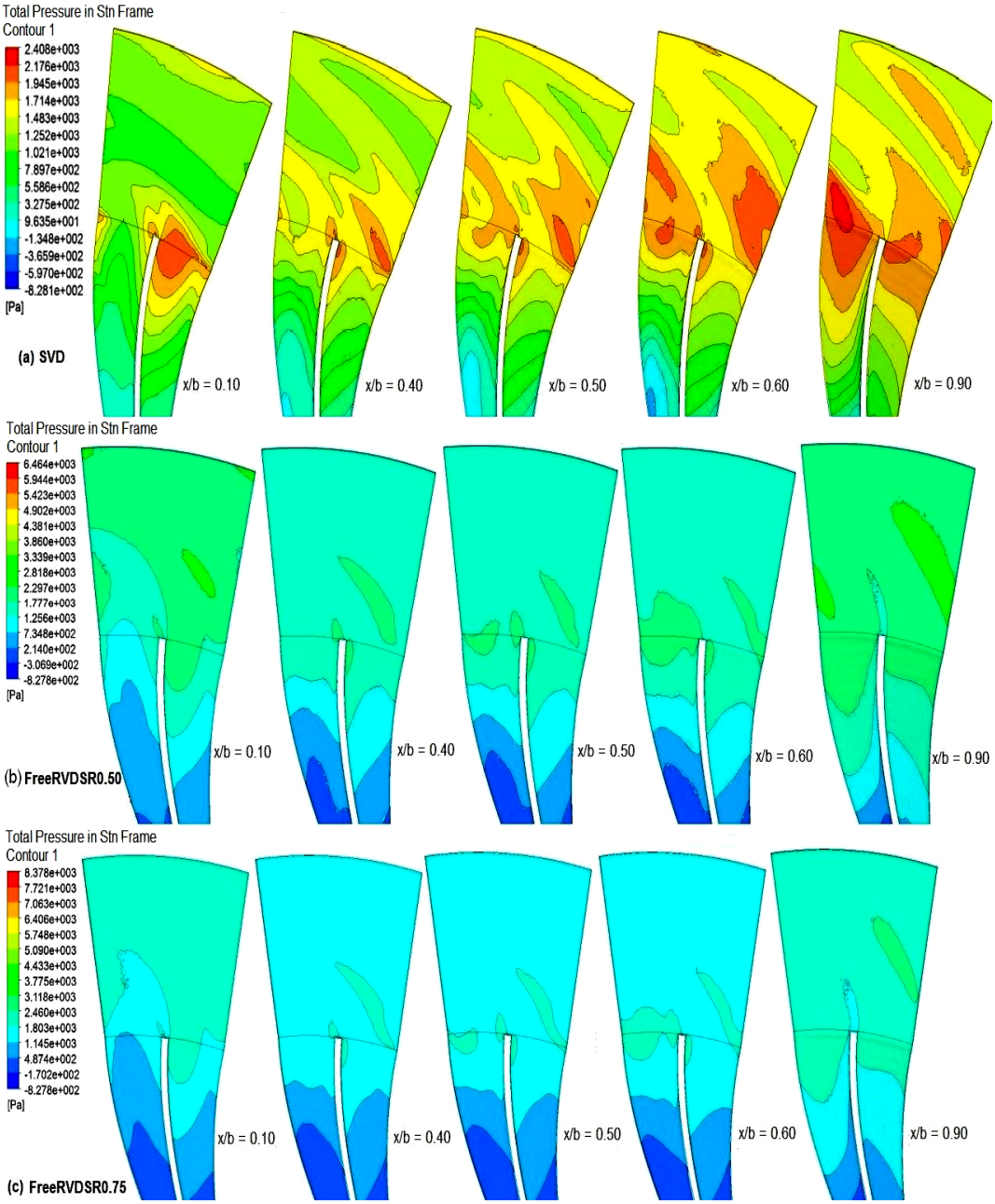

Fig. 13. Distribution of stagnation pressure axially from hub to shroud at Φ = 0.275 for FreeRVD and SVD configurations.

3.2 Comparison of Various Free Rotating Vaneless Diffusers with Forced Rotating Vaneless Diffuser

The configuration, FreeRVDSR1.0 shown in various figures in this present study represents a compressor stage with forced type of rotating vaneless diffuser (Seralathan Sivamani and Roy Chowdhury 2016). This forced type of rotating vaneless diffuser is equivalent to an extension of impeller disks alone by 40% of impeller's exit diameter (D_2) without affecting the blade tip geometry (Seralathan Sivamani and Roy Chowdhury 2016). An attempt is made here by comparing the performances of a compressor stage with different free type of rotating vaneless diffusers, forced type of rotating vaneless diffuser and conventional stationary vaneless diffuser.

The efficiency of FreeRVDSR1.0 is lesser compared to SVD but higher in comparison with various FRVD configurations at design flow rates and at all above off-design flow rates except Φ = 0.371. As the total temperature of fluid observed at stage exit is comparatively lesser for FreeRVDSR1.0, its efficiency is better compared to all free rotating vaneless diffusers. Energy coefficient, a pointer towards energy acquired by the fluid within the compressor stage is higher in FreeRVDSR1.0 in comparison with SVD, but lower

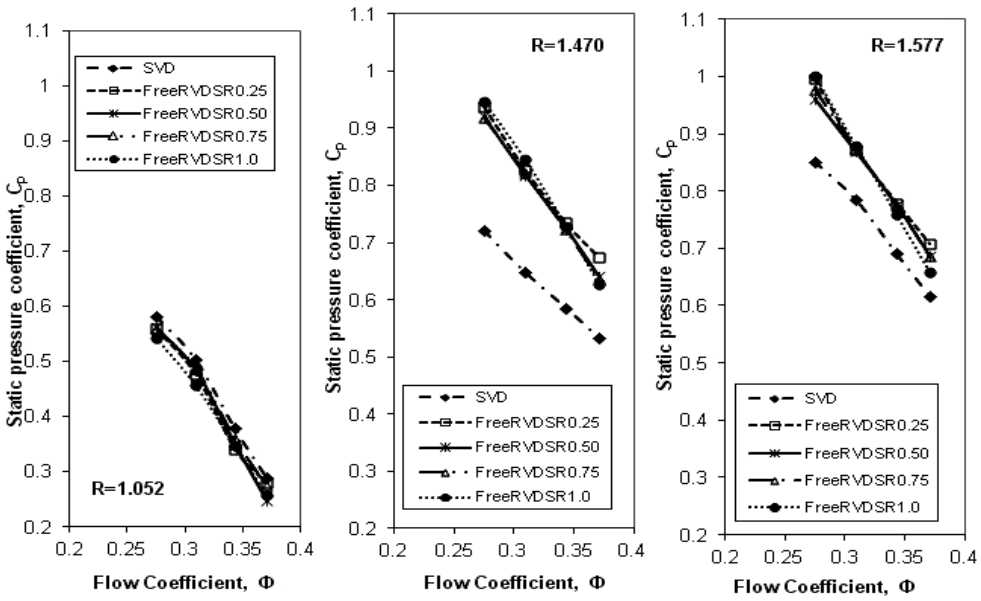

Fig. 14. Variations of static pressure coefficient for different diffuser configurations.

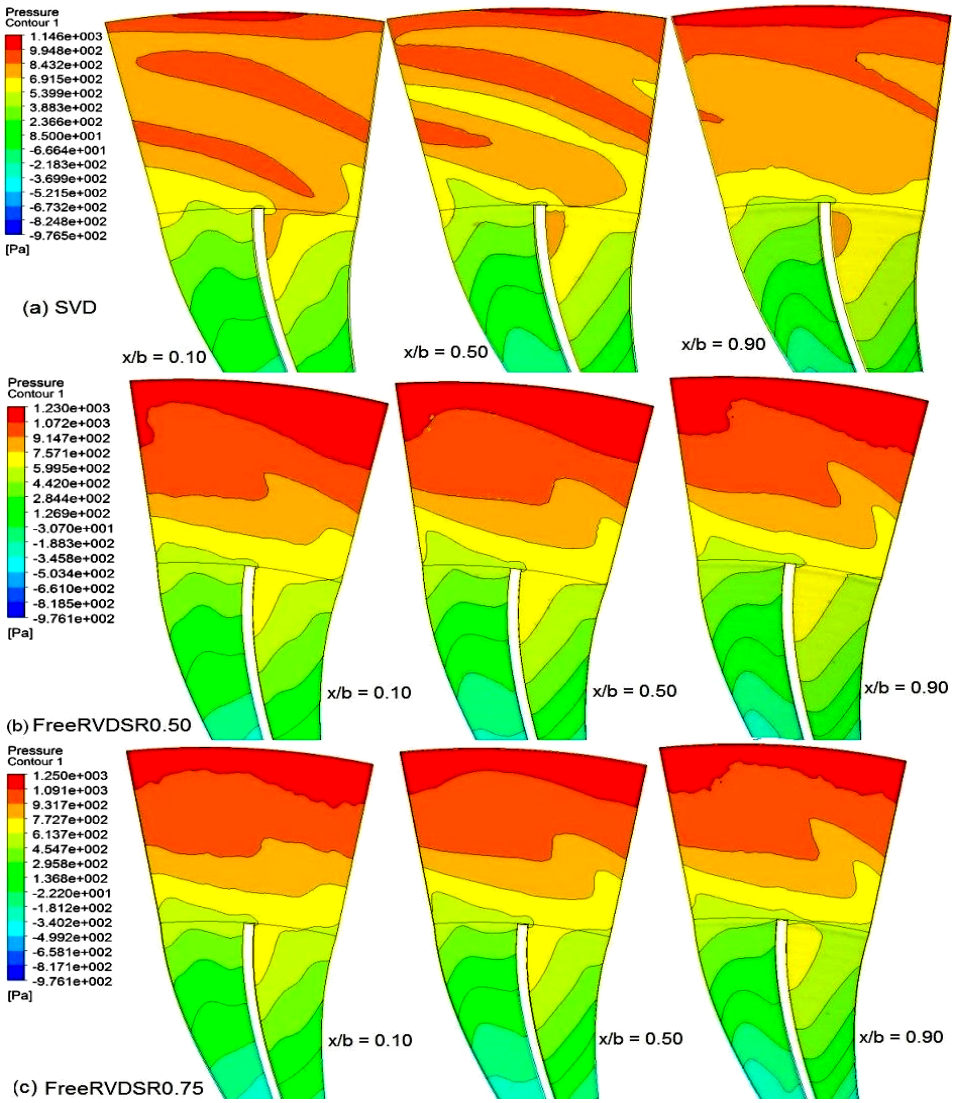

Fig. 15. Distribution of static pressure axially from hub to shroud at Φ = 0.275 for different diffuser configurations.

compared to various FRVD configurations at all flow rates. Recovery of static pressure in FreeRVDSR1.0 is higher at Φ = 0.275 and 0.309 but, it is lower at Φ = 0.343 and 0.371 in comparison with various free rotating vaneless diffusers. There is a net gain in total pressure for FreeRVDSR1.0 after overcoming the losses within the diffuser passage at Φ = 0.275 and 0.309. However, there is a minor stagnation pressure loss at Φ = 0.371 with neither loss nor gain at flow coefficient Φ = 0.343. But, all the free rotating vaneless diffusers reported only a varying net gain in stagnation pressures based on rotational speed ratios. The variation of flow angle for FreeRVDSR1.0 is in similar pattern with free rotating vaneless diffusers by having smaller flow angles at all flow rates. This results in substantial reduction of the frictional losses by having a shorter flow path length. In both free and forced rotating vaneless diffusers, added work input is made by causing the walls of vaneless diffuser to rotate at certain speed with respect to impeller's rotational speed. This results in addition of energy to the fluid. The absolute velocity distribution of FreeRVDSR1.0, as seen in Fig. 7 at R = 1.577, is lesser compared to various free rotating vaneless diffusers. It is interesting to note that absolute velocities of various free rotating vaneless diffusers realized at R = 1.577 increases depending upon the speed ratios of free rotating vaneless diffusers. By comparing FreeRVDSR1.0 with various FRVDs as seen in Fig. 7 at radius ratio R = 1.577, it is observed that the actual work input given to FreeRVDSR1.0 is lesser. This may be due to comparatively higher disk friction losses in FreeRVDSR1.0. Also, it is known that the disk friction losses decrease with increase in mass flow rate. Therefore, the energy level realized by the fluid with rise in kinetic energy after overcoming the losses within the diffuser passage is lower compared to various free rotating vaneless diffusers but better compared to SVD. Based on the stagnation pressure distribution as seen in Fig. 12, the diffusion process in FreeRVDSR1.0 is better compared to SVD but not as effective compared to various free rotating vaneless diffusers. The stagnation pressure distribution of FreeRVDSR1.0 is higher than SVD but lesser compared to various free rotating vaneless diffusers. It is lesser by 19.98% at design flow coefficient and by 18.82% to 17.92% at above off-design flow coefficients compared to FreeRVDSR0.75.

The static pressure distribution pattern of FreeRVDSR1.0 is higher compared to SVD and nearly same as various free rotating vaneless diffusers at all mass flow rates. Based on this comparative study between various free type of rotating vaneless diffusers and forced type of rotating vaneless diffuser, it is understood that optimum rotational speed of the rotating vaneless diffuser plays an important role in facilitating the effective diffusion process within the diffuser passage and thereby enhancing the overall compressor performance.

4. CONCLUSION

The stationary vaneless diffuser section of a centrifugal compressor stage is completely replaced with a rotating vaneless diffuser rotating at different rotational speeds. Based on the numerical studies, the following conclusions are drawn:

Four different rotational speeds are selected for the rotating vaneless diffuser. Free type rotating vaneless diffusers are rotated at speed ratios SR0.25, SR0.50 and SR0.75. The total temperature of fluid at compressor stage exit increases with increase in rotational speed ratios of free rotating vaneless diffuser section. This affects the efficiency. Among all the FRVD configurations, FreeRVDSR0.75 records the least value. Efficiencies of FreeRVDSR0.50 and FreeRVDSR0.75 are nearly identical but lesser than FreeRVDSR0.25 by 0.90% to 1.98%. Energy coefficient of FreeRVDSR0.75 is highest among all the FRVD configurations by 38.10% to 46.04% compared to SVD. Within diffuser passage, the frictional losses between the flow and rotating walls of FRVDs are much reduced. FreeRVDSR0.75 has the lowest flow angles and FreeRVDSR0.25 has the highest. However, these flow angles are lesser compared to SVD which results in a shorter flow path length thereby reducing the frictional losses substantially. In all free rotating vaneless diffusers, only gain in stagnation pressure is observed. This net gain in stagnation pressure achieved is due to the energy added to the fluid by the rotating walls of FRVD. The rotational speed of FRVD determines the extent of net gain in energy level attained by the fluid and the drop in stagnation pressure losses. The net gain in energy level raises the kinetic energy level of the fluid. A closer look into the absolute velocity contours reveals the extent of fluid getting energized and FreeRVDSR0.75 is energized to the maximum extent. Due to the effective diffusion process, this results in raising the values of static and stagnation pressures at exit. On a closer look into static pressure distribution along with the distribution of stagnation pressure at stage exit, it is established that FreeRVDSR0.75 undergoes a comparatively better diffusion process among all the FRVD contafigurations. The efficacy of diffusion process in a compressor stage with FRVD is better at speed ratio above SR0.50.

Later, the speed ratio of rotating vaneless diffuser is increased to SR1.0 to make it behave like a forced type and its performance is compared with various free rotating vaneless diffuser configurations.

Based on this study, it is understood that an optimum rotational speed of the rotating vaneless diffuser plays an important role in facilitating the effective diffusion process within the diffuser passage.

REFERENCES

Castaing, R. and Y. Ribaud (1972, May). Improvements to centrifugal compressors.

French patent registration number 2, 187-031 (in French).

Fradin, C. (1975). The effect of the rotational speed of a vaneless diffuser on the performance of a centrifugal compressor. *Report No. ESA-TT-202.*

Govardhan, M., B. S. N. Moorthy and G. Gopalakrishnan (1978). A preliminary report on the rotating vaneless diffuser for a centrifugal impeller. In *Proceedings of the First International Conference on Centrifugal Compressor Technology*, Indian Institute of Technology Madras, Chennai, India, 5 .

Novak, J. (1907). Glatter diffuser bei zentrifugal pumpen, Vaneless diffuser in centrifugal pumps, Zeitschrift fuer das gesamte Turbinenwesen Heft 24.

Rodgers, C. (1972). Analytical experimental and mechanical evaluation of free rotating vaneless diffuser, Final report, ER 2391, *AD 744475*.

Rodgers, C. (1974). Continued testing – MERDC rotating diffuser compressor, *ADA018160*.

Rodgers, C. (1976). Design and test of an experimental rotating diffuser centrifugal compressor test rig. *SAE 760927*, 17 pages.

Rodgers, C. and H. Mnew (1970). Rotating vaneless diffuser study, *AD 716370*.

Rodgers, C. and H. Mnew (1974). Experiments with a model free rotating vaneless diffuser. In *Proceedings of the ASME Gas Turbine Conference and Products Show*, Zurich, Switzerland, 12 pages.

Rodgers, C. and H. Mnew (1975). Experiments with a model free rotating vaneless diffuser. *ASME Journal of Engineering for Power*, 231-244.

Rodgers, C. and L. Blinman (1977). Test evaluation of stationary and rotating diffusers for high pressure ratio radial compressor, *ADA049856*.

Seralathan, S. and D. G. Roy Chowdhury (2016). Performance of a low pressure ratio centrifugal compressor stage with a rotating vaneless diffuser by impeller disk extended shrouds. *Journal of Applied Fluid Mechanics* 9(6), 2933-2947.

Seralathan, S. and D. G. Roy Chowdhury (2014b). Performance enhancement of the centrifugal compressor stage with a rotating vaneless diffuser – a numerical study. In *Proceedings of the ASME 2014 Gas Turbine India Conference*, New Delhi, India, GTINDIA2014-8179, 10 .

Seralathan, S. and D. G. Roy Chowdhury (2014a). Free rotating vaneless diffuser of diffuser diameter ratio 1.30 with different speed ratios and its effect on centrifugal compressor performance improvement. *Energy Procedia* 54, 506-517.

Seralathan, S. and D. G. Roy Chowdhury (2015). Numerical study on the effect of free rotating vaneless diffuser of exit diameter to inlet diameter ratio 1.3 with speed ratio 0.50 on centrifugal compressor performance. *Applied Mechanics and Materials* 813-814, 1063-1069.

Yves, R, and C. Fradin (1989). Revaluation of researches on the free rotating vaneless diffuser. In *Proceedings of the ASME International Gas Turbine and Aero-engine Congress and Exposition*, 89-GT-224.